Research in Astron. Astrophys. **2009** Vol. **9** No. **2**, 168–178
http://www.raa-journal.org *http://www.iop.org/journals/raa*

***R**esearch in*
***A**stronomy and*
***A**strophysics*

The debeamed luminosity, sychrotron peak frequency and black hole mass of BL Lac objects *

Zhong-Zu Wu[1,2,3], Min-Feng Gu[1,2] and Dong-Rong Jiang[1,2]

[1] Shanghai Astronomical Observatory, Chinese Academy of Sciences, Shanghai 200030, China; *zzwu@shao.ac.cn*
[2] Joint Institute for Galaxy and Cosmology (JOINGC) of SHAO and USTC
[3] NAOC-GZU Sponsored Center for Astronomy, Guizhou Univ., Guiyang 550025, China

Received 2008 January 30; accepted 2008 April 7

Abstract We estimate the intrinsic luminosities and synchrotron peak frequencies using the derived Doppler factor for a sample of 170 BL Lac objects, of which the synchrotron peak frequency is derived by fitting the SED constructed with the collected multi-band data from the literature. We find that the debeamed radio and optical core luminosities follow the same correlation found for FR I radio galaxies, which is in support of the unification of the BL Lac objects and the FR I galaxies based on orientation. For the debeamed luminosity at the synchrotron peak frequency, we find a significant positive correlation between the luminosity and intrinsic synchrotron peak frequency. This implies that the more powerful sources may have the majority of jet emission at higher frequency. At the synchrotron peak frequency, the intrinsic luminosity and black hole mass show strong positive correlation, while mild correlation is found in the case of jet power, indicating that the more powerful sources may have more massive black holes.

Key words: black hole physics — BL Lacertae objects: general — galaxies: active — galaxies: jets — galaxies: nuclei

1 INTRODUCTION

BL Lac objects are one of the extreme classes of active galactic nuclei (AGN) with few if any emission lines, but they have strong highly variable and polarized non-thermal continuum emission ranging from radio to γ-ray bands. Traditionally, they have been divided into radio-selected and X-ray-selected BL Lac objects (RBLs and XBLs, respectively) based on the surveys where they were primarily discovered. In recent years, the dichotomy has been replaced by a more physically meaningful classification based upon the overall spectral energy distribution (SED) of the object, namely, low frequency peaked BL Lac objects (LBL), intermediate objects (IBL) and high frequency peaked BL Lac objects (HBL) (Padovani & Giommi 1995). Generally, RBLs tend to be LBLs, and XBLs tend to be HBLs (see review by Urry & Padovani 1995). The synchrotron peak frequency of RBLs is usually in the radio/IR band, while it is in the UV/X-ray band for XBLs (Giommi et al. 1995). The recent studies of the SED of large samples of BL Lac objects showed that BL Lac objects most likely form one class with a continuous distribution of synchrotron emission peak energies, while RBLs and XBLs represent the opposite ends of the continuum (Nieppola et al. 2006).

* Supported by the National Natural Science Foundation of China.

Fossati et al. (1998) and Ghisellini et al. (1998) have proposed the so-called 'blazar sequence' with plots of various powers vs. synchrotron peak frequencies $\nu_{\rm peak}$ for a sample of blazars containing flat-spectrum radio quasars (FSRQ) and BL Lac objects, of which an anti-correlation was apparent, with the most powerful sources having relatively low synchrotron peak frequencies and the least powerful ones having the highest $\nu_{\rm peak}$. The theoretical interpretation of this anti-correlation was proposed by Ghisellini et al. (1998): the more powerful sources suffered a larger probability of losing energy and therefore are subjected to more cooling and thus translate into a lower value of $\nu_{\rm peak}$. However, recent studies have largely changed this scenario. Recently, Nieppola et al. (2006) proposed that there are anti-correlations between the luminosities at 5 GHz, 37 GHz, and 5500 Å and $\nu_{\rm peak}$ for a large sample of BL Lac objects, while based on all the correlations with $\nu_{\rm peak}$, they concluded that the blazar sequence scenario is not valid. By estimating the Doppler factor for a sample of 170 BL Lac objects selected from Nieppola et al. (2006), Wu et al. (2007) found a significant anti-correlation between the total 408 MHz luminosity, which is supposed to be intrinsic, and the intrinsic $\nu_{\rm peak}$, with a large scatter which, however, undermines the 'blazar sequence'. Moreover, the evidence of low-power LBLs has been recently discovered (Padonavi et al. 2003; Caccianiga & Marchã 2004; Antón & Browne 2005), and the possible discovery of high luminosity HBLs is also reported in the Sedentary survey (Giommi et al. 2005). In addition, the high-power-high-$\nu_{\rm peak}$ FSRQs were found in the Deep X-ray Radio Blazar Survey (DXRBS), which is selected from both X-ray and radio, though they do not reach the extreme $\nu_{\rm peak}$ values of HBLs. From all these discoveries, it seems that the blazar sequence in its simplest form cannot be valid (Padovani 2006). Currently, what are the main physical parameters that determine the shift in the synchrotron peak frequency of BL Lac objects still seems unclear.

According to the unified scheme for AGNs, BL Lac objects are thought to be low-luminosity radio galaxies viewed at relatively small angles to the line of sight and the relativistic beaming has enormous effects on the observed luminosities. Generally, the intrinsic (debeamed) luminosity emitted from a jet in BL Lac objects can be estimated using the Doppler factor and assuming the jet geometry. Using the empirical relation of Giovannini et al. (2001), Wu et al. (2007) estimated the Doppler factor for a sample of 170 BL Lac objects with the observed radio core observed either with VLA or MERLIN. In this paper, we will correct the beaming effect in the multi-band luminosity and the synchrotron peak frequency directly using the derived Doppler factor of Wu et al. (2007) for the same sample. Our aim is mainly to investigate the correlation between the luminosity at synchrotron peak frequency and the synchrotron peak frequency after eliminating the beaming effect. The layout of this paper is as follows. The sample is given in Section 2. In Section 3, the various correlation analyses are presented, which involve the multi-band luminosity, the synchrotron peak frequency, as well as the black hole mass. The discussions are shown in Section 4, and the results are summarized in Section 5. Throughout the work, we adopt the following values for the cosmological parameters: $H_0 = 70\,{\rm km\,s^{-1}\,Mpc^{-1}}$, $\Omega_{\rm M} = 0.3$, and $\Omega_\Lambda = 0.7$, except as otherwise stated. The spectral index α is defined as $f_\nu \propto \nu^{-\alpha}$.

2 THE SAMPLE

Nieppola et al. (2006) presented a large sample of BL Lac objects from the Metsähovi radio observatory BL Lac sample consisting of 381 objects selected from the Veron-Cetty & Veron BL Lac Catalog (Veron-Cetty & Veron 2000), and 17 objects from the literature, of which many sources are from the well-known BL Lac samples such as 1Jy, S4, S5, Einstein Medium Sensitivity Survey (EMSS), Einstein Slew Survey, and DXRBS. The authors argued that this sample is supposed to have no selection criteria (other than declination) in addition to the ones in the original surveys. From this sample, Wu et al. (2007) estimated the Doppler factor for a sample of 170 BL Lac objects using the radio core emission from either VLA or MERLIN observations. The sample investigated in this paper is the same as that in Wu et al. (2007), i.e. 170 BL Lac objects with estimated δ. The Doppler factor was estimated using the correlation found by Giovannini et al. (2001) for radio galaxies,

$$\log\ P_{\rm ci5} = \ 0.62 \log\ P_t + 8.41, \tag{1}$$

where $P_{\rm ci5}$ is the intrinsic core radio power at 5 GHz derived assuming $\Gamma = 5$ (see Giovannini et al. 2001, for details), and $P_{\rm t}$ is the total radio power at 408 MHz. From the measured total 408 MHz radio power, we can obtain the intrinsic core radio power. Thus, the Doppler factor can be obtained from $P_{\rm co5} = P_{\rm ci5}\delta^{2+\alpha}$ (corresponding to a continuous jet), assuming $\alpha = 0$, where $P_{\rm co5}$ is the observed 5 GHz core luminosity (see Wu et al. 2007, for details).

To construct the SED for all 170 BL Lac objects, we collected the radio, optical and X-ray data from the NASA/IPAC Extragalactic Database (NED), the Astrophysical Catalogs Support System (CATs) maintained by the Special Astrophysical Observatory, Russia, and the catalog of integral blazar working group (IBWG)[1]. The R-band core luminosities were mainly obtained from Urry et al. (2000), O'Dowd & Urry (2005) and Nilsson et al. (2003). The X-ray data were collected from Laurent-Muehleisen et al. (1999), Donato et al. (2001), Rector & Stocke (2000), Reich et al. (2000), Turriziani et al. (2007), and RBSC-NVSS (2000). The Galactic extinction in the optical band was corrected using the value from NED. Following Nieppola et al. (2006), the SED of each source was constructed in the $\log\nu - \log\nu F_\nu$ representation in the observer's frame, based on the multi-frequency data. The synchrotron component of the SED was fitted with a parabolic function $y = Ax^2 + Bx + C$, therefore, the synchrotron peak frequency in the rest frame was obtained as $\nu_{\rm peak} = -B(1+z)/2A$, in which z is the redshift.

In principle, whether or not to include X-ray data in the fit can be decided based on the X-ray spectral index fitted from high quality X-ray spectra. An X-ray spectral index of $\alpha > 1$ means a synchrotron origin of X-ray emission, while $\alpha < 1$ indicates an origin of the inverse Compton process, which implies that the X-ray data should be excluded from the fit. Unfortunately, most of the sources in our sample have no well-measured X-ray spectral index, which precludes us from doing so. Tentatively in this work, whether or not include X-ray data in the fit was decided solely based on a visual inspection on the SED of each object. Similar to Wu et al. (2007), the objects were assigned an LBL/IBL/HBL classification based on $\nu_{\rm peak}$: for LBLs $\log\nu_{\rm peak} < 14.5$, for IBLs $14.5 < \log\nu_{\rm peak} < 16.5$, and for HBLs $\log\nu_{\rm peak} > 16.5$.

We estimated the jet power using the formula derived from Punsly (2005):

$$Q_{\rm jet} = 5.7\times10^{44}(1+z)^{1+\alpha}Z^2F_{151}\ \ {\rm erg\,s^{-1}}, \quad (2)$$

$$Z \approx 3.31 - 3.65\times[(1+z)^4 - 0.203(1+z)^3 + 0.749(1+z)^2 + 0.444(1+z) + 0.205]^{-0.125}, \quad (3)$$

where F_{151} is the optically thin flux density from the lobes measured at 151 MHz in units of janskys, and the value of $\alpha \approx 1$ is a good fiducial value (see Punsly 2005, for more details). We calculated the F_{151} through the extrapolation either from the extended radio flux at 5 GHz or 1.4 GHz, or from the low frequency total radio flux assuming $\alpha = 1.0$.

To estimate the black hole mass, we collected the R-band magnitudes of host galaxies for 121 sources, of which the core R-band magnitude were also available. Following Wu et al. (2007), we adopted the average redshift of the classification (i.e. LBLs, IBLs and HBLs) for sources without redshift. The sample is listed in Table 1.

3 CORRELATION ANALYSIS

It is commonly accepted that the luminosity of blazars is dominated by the emission from jets, which is Doppler boosted. Using the Doppler factor derived in Wu et al. (2007) and assuming the same Doppler factor at various wavebands of synchrotron emission as suggested by Capetti et al. (2002) and Trussoni et al. (2003), we calculate the intrinsic luminosity using $L_{\rm int} = L_{\rm obs}/\delta^{2+\alpha}$ (corresponding to a continuous jet), in which $L_{\rm int}$ is the intrinsic luminosity, and $L_{\rm obs}$ is the observed luminosity. Since the synchrotron peak frequency $\nu_{\rm peak} \propto B\delta\gamma^2_{\rm peak}$, the intrinsic one $\nu'_{\rm peak}$ can be obtained as $\nu_{\rm peak}/\delta$, which is only dependent on B and $\gamma_{\rm peak}$, where B is the strength of the magnetic field, δ the Doppler factor, and $\gamma_{\rm peak}$ a characteristic electron energy that is determined by a competition between accelerating and cooling processes. With these intrinsic parameters, we explore various correlations below.

[1] *http://altamira.asu.cas.cz/iblwg/catalog.php*

Table 1 The Sample

IAU name	Source	z	$\log \nu'_{\rm peak}$	$\log \nu L_{\nu \rm p}$	$\log Q_{\rm jet}$	δ	$m_{\rm h}$	Refs.	$\log M_{\rm bh}$
(1)	(2)	(3)	(4)	(5)	(6)	(7)	(8)	(9)	(10)
0006−063	NRAO 5	0.347	12.17	45.44	44.79	5.97	...	...	...
0007+472	RX J0007.9+4711	0.280	14.75	44.62	43.37	2.71	>19.01	1	7.93
0035+598	1ES 0033+595	0.086	17.01	44.58	41.87	2.33	>17.56	2	7.25
0040+408	1ES 0037+405	0.271	18.17	44.99	42.79	1.92	...	...	...
0050−094	PKS 0048−097	0.216	12.89	45.13	44.22	3.29	...	...	...
0110+418	NPM1G +41.0022	0.096	15.23	44.05	42.70	1.06	15.28	1	8.51
0112+227	S2 0109+22	0.473	12.92	46.23	44.17	8.50	...	...	...
0115+253	RXS J0115.7+2519	0.350	13.47	44.80	43.59	2.59	17.91	1	8.76
0123+343	1ES 0120+340	0.272	17.99	45.51	42.72	2.93	17.41	3	8.69
0124+093	MS 0122.1+0903	0.339	15.61	44.38	41.43	1.96	18.20	4	8.57
0136+391	B3 0133+388	0.271	16.20	45.75	43.29	2.44	...	...	...
0141−094	PKS 0139−09	0.733	13.19	46.06	45.03	7.43	>18.09	4	9.63
0148+140	1ES 0145+138	0.125	15.86	43.94	42.01	0.54	16.67	2	8.12
0153+712	8C 0149+710	0.022	14.72	44.03	41.86	1.29	11.68	1	8.65
0201+005	MS 0158.5+0019	0.299	17.85	45.27	42.32	2.30	17.84	2	8.59
0208+353	MS 0205.7+3509	0.318	15.18	44.73	41.76	2.75	...	...	...
0214+517	87GB 02109+5130	0.049	15.51	44.12	42.33	1.50	13.56	3	8.60
0222+430	3C 66A	0.440	14.84	46.25	45.41	3.85	...	...	...
0232+202	1ES 0229+200	0.140	16.48	44.96	43.04	1.93	15.34	2	8.92
0238+166	AO 0235+164	0.940	12.68	46.87	45.09	10.78	>17.18	4	10.42
0301+346	MS 0257.9+3429	0.245	13.29	44.78	42.34	1.90	17.18	2	8.68
0314+247	RXS J0314.0+2445	0.054	13.36	44.47	41.25	0.97	15.65	1	7.67
0326+024	2E 0323+0214	0.147	15.87	44.72	42.01	2.07	16.59	1	8.36
0416+010	2E 0414+0057	0.287	16.42	45.57	43.98	2.13	16.83	2	9.05
0422+198	MS 0419.3+1943	0.512	16.10	45.44	43.01	2.32	18.78	2	8.81
0424+006	PKS 0422+004	0.310	14.88	45.71	44.15	6.24	...	...	...
0505+042	RXS J0505.5+0416	0.027	15.62	42.76	41.89	1.20	17.81	1	5.81
0507+676	1ES 0502+675	0.314	18.04	45.94	42.05	5.62	...	...	...
0508+845	S5 0454+84	0.112	12.83	44.07	41.62	10.76	>21.99	2	5.33
0509−040	4U 0506−03	0.304	18.39	45.39	43.42	1.93	17.76	2	8.66
0613+711	MS 0607.9+7108	0.267	14.48	44.84	41.89	3.49	17.00	2	8.87
0625+446	87GB 06216+4441	0.473	13.36	45.69	44.53	5.46	...	...	...
0650+250	1ES 0647+250	0.203	15.51	45.57	42.71	3.24	>18.61	2	7.73
0654+427	B3 0651+428	0.126	14.98	44.51	42.93	2.38	15.59	1	8.67
0656+426	NPM1G +42.0131	0.059	15.41	44.14	43.73	0.86	13.63	1	8.78
0710+591	EXO 0706.1+5913	0.125	16.85	44.66	42.85	1.87	15.57	1	8.67
0721+713	S5 0716+714	0.300	14.30	45.99	44.35	3.23	>19.55	2	7.74
0738+177	PKS 0735+17	0.424	12.82	46.38	43.28	29.41	>19.75	2	8.08
0744+745	MS 0737.9+7441	0.315	14.52	45.12	42.60	3.05	17.55	2	8.81
0753+538	S4 0749+54	0.200	12.36	44.81	43.26	9.26	>21.44	2	6.30
0757+099	PKS 0754+100	0.266	13.00	45.74	43.11	17.72	>18.31	2	8.21
0806+595	SBS 0802+596	0.300	15.31	45.28	43.04	2.36	16.63	1	9.20
0809+523	1ES 0806+524	0.137	16.14	45.04	42.69	3.32	15.83	3	8.65
0818+423	OJ 425	0.530	12.55	45.53	45.05	6.33	>20.47	2	8.01
0823+223	4C 22.21	0.951	12.87	45.88	46.38	2.73	>19.10	4	9.47
0825+031	PKS 0823+033	0.506	11.84	45.94	43.08	29.42	>19.28	2	8.55
0831+044	PKS 0829+046	0.174	13.07	45.24	43.56	6.21	16.66	2	8.52
0831+087	1H 0827+089	0.941	14.00	45.35	44.95	4.04	...	...	...
0832+492	OJ 448	0.548	12.38	45.46	43.84	8.39	>19.26	2	8.66
0854+441	US 1889	0.382	15.04	45.19	43.90	1.79	...	...	...
0854+201	OJ 287	0.306	12.33	46.09	43.10	17.87	>18.08	2	8.50
0915+295	B2 0912+29	0.302	15.39	45.32	44.01	2.96	...	...	...
0916+526	RXS J0916.8+5238	0.190	15.36	44.40	43.55	1.85	15.95	1	8.98
0929+502	RXS J0929.2+5013	0.370	13.33	45.45	43.86	9.23	...	...	...
0930+498	1ES 0927+500	0.188	17.33	44.96	41.85	2.70	17.36	2	8.26
0930+350	B2 0927+35	0.302	12.81	44.52	44.29	3.68	...	...	...
0952+656	RGB J0952+656	0.302	14.96	44.83	43.24	1.99	...	...	...
0954+492	MS 0950.9+4929	0.380	17.25	45.08	42.06	2.12	...	...	...
0958+655	S4 0954+65	0.368	13.54	45.76	43.51	6.79	>18.81	2	8.37

Table 1 —Continued.

IAU name	Source	z	log $\nu'_{\rm peak}$	log $\nu L_{\nu \rm p}$	log $Q_{\rm jet}$	δ	$m_{\rm h}$	Refs.	log $M_{\rm bh}$
(1)	(2)	(3)	(4)	(5)	(6)	(7)	(8)	(9)	(10)
1012+424	RXS J1012.7+4229	0.364	18.24	45.55	43.69	1.92	17.61	1	8.96
1015+494	GB 1011+496	0.200	16.27	45.14	43.61	2.59	16.15	3	8.94
1031+508	1ES 1028+511	0.360	16.71	45.79	43.10	3.39	18.10	3	8.70
1037+571	RXS J1037.7+5711	0.302	14.40	45.37	43.71	3.70	...	...	...
1047+546	1ES 1044+549	0.473	12.83	45.46	42.96	2.05	19.31	2	8.44
1053+494	MS 1050.7+4946	0.140	14.99	44.25	42.16	2.49	15.12	1	9.03
1104+382	MRK 421	0.030	16.40	44.67	42.27	1.99	13.22	2	8.23
1109+241	1ES 1106+244	0.460	16.57	45.25	43.78	2.42	18.86	2	8.64
1120+422	EXO 1118.0+4228	0.124	16.33	44.26	42.38	1.76	...	...	...
1136+701	MRK 180	0.045	16.86	44.15	43.02	0.78	14.37	2	8.10
1136+676	RXS J1136.5+6737	0.134	15.40	44.50	41.95	2.64	15.76	3	8.66
1149+246	EXO 1449.9+2455	0.402	17.13	45.39	43.60	2.20	18.12	1	8.83
1150+242	B2 1147+245	0.200	13.29	44.92	43.15	7.11	$>$20.40	2	6.82
1151+589	RXS J1151.4+5859	0.302	15.43	45.04	43.79	2.58	...	...	...
1209+413	B3 1206+416	0.302	13.54	45.22	43.50	6.70	...	...	...
1215+075	1ES 1212+078	0.136	14.68	44.60	43.13	2.49	15.81	2	8.65
1217+301	B2 1215+30	0.130	14.69	44.59	43.28	3.39	15.78	2	8.61
1220+345	GB2 1217+348	0.643	13.63	45.84	44.42	5.80	...	...	...
1221+301	PG 1218+304	0.182	17.16	45.36	42.65	2.60	16.86	2	8.47
1221+282	ON 231	0.102	14.45	44.65	42.99	5.32	16.43	2	8.01
1223+806	S5 1221+80	0.473	14.23	45.29	44.77	4.32	...	...	...
1224+246	MS 1221.8+2452	0.218	13.43	44.73	42.11	2.96	18.32	2	7.96
1230+253	RXS J1230.2+2517	0.135	14.11	44.76	43.08	3.60	...	...	...
1231+642	MS 1229.2+6430	0.163	15.19	44.60	42.18	2.96	16.15	2	8.70
1237+629	MS 1235.4+6315	0.297	15.07	44.70	42.24	3.02	...	...	...
1241+066	1ES 1239+069	0.150	18.68	44.49	41.33	2.45	$>$22.08	2	5.63
1248+583	PG 1246+586	0.847	14.17	46.80	44.70	11.10	$>$19.43	2	9.15
1253+530	S4 1250+53	0.302	14.64	44.92	44.26	3.52	...	...	...
1257+242	1ES 1255+244	0.141	16.70	44.86	42.29	1.30	16.53	2	8.33
1310+325	AUCVn	0.996	12.61	47.10	44.38	27.73	$>$17.93	4	10.12
1322+081	1ES 1320+084N	1.500	13.14	46.91	44.41	4.09	$>$18.71	2	10.28
1341+399	RXS J1341.0+3959	0.163	18.21	44.74	43.05	1.44	15.82	1	8.86
1402+159	MC 1400+162	0.244	16.24	45.03	44.40	1.90	...	...	...
1404+040	MS 1402.3+0416	0.344	15.36	45.42	43.62	1.64	$>$18.87	2	8.26
1409+596	MS 1407.9+5954	0.496	15.81	44.97	43.35	2.55	18.25	2	9.04
1415+485	RGB J1415+485	0.496	14.16	45.05	43.50	4.06	19.30	1	8.51
1415+133	PKS 1413+135	0.247	12.08	45.00	44.52	3.47	...	...	...
1417+257	2E 1415+2557	0.237	17.17	45.35	43.57	2.13	16.28	3	9.09
1419+543	OQ 530	0.152	12.93	45.11	42.53	11.38	15.90	2	8.74
1427+238	PKS 1424+240	0.160	15.22	45.10	43.55	2.66	$>$20.67	2	6.42
1427+541	RGB J1427+541	0.106	14.13	44.18	42.17	1.38	14.81	1	8.86
1428+426	H 1426+428	0.129	18.19	45.06	42.22	1.56	15.97	2	8.51
1439+395	PG 1437+398	0.344	16.07	45.32	43.83	1.87	17.48	2	8.95
1442+120	1ES 1440+122	0.163	15.81	44.74	43.10	2.06	16.45	2	8.55
1444+636	MS 1443.5+6349	0.298	16.58	44.48	42.17	1.69	...	...	...
1448+361	RXS J1448.0+3608	0.271	14.90	45.16	43.31	2.51	...	...	...
1458+373	B3 1456+375	0.333	12.85	44.93	43.76	5.39	...	...	...
1501+226	MS 1458.8+2249	0.235	14.46	44.97	42.59	4.59	17.40	2	8.52
1509+559	SBS 1508+561	2.025	14.21	47.38	44.61	5.03	...	...	...
1516+293	RXS J1516.7+2918	0.130	14.82	44.37	42.87	1.29	15.52	1	8.75
1517+654	1H 1515+660	0.702	17.04	46.63	43.50	3.32	$>$18.51	2	9.36
1532+302	RXS J1532.0+3016	0.064	15.01	44.10	42.17	1.66	14.86	1	8.26
1533+342	RXS J1533.4+3416	0.810	15.42	45.97	43.55	4.86	...	...	...
1534+372	RGB J1534+372	0.143	13.82	44.22	41.81	2.21	16.97	1	8.13
1535+533	1ES 1533+535	0.890	18.49	46.44	44.24	2.55	$>$17.44	4	10.21
1536+016	MS 1534.2+0148	0.312	17.19	44.85	43.39	1.89	17.62	2	8.76
1540+819	1ES 1544+820	0.271	15.63	45.12	43.21	2.30	$>$19.14	2	7.82
1540+147	4C 14.6	0.605	13.54	45.83	45.43	6.34	18.76	1	9.04
1542+614	RXS J1542.9+6129	0.302	13.90	45.25	43.06	4.42	...	...	...

Table 1 —Continued.

IAU name (1)	Source (2)	z (3)	log $\nu'_{\rm peak}$ (4)	log $\nu L_{\nu \rm p}$ (5)	log $Q_{\rm jet}$ (6)	δ (7)	$m_{\rm h}$ (8)	Refs. (9)	log $M_{\rm bh}$ (10)
1554+201	MS 1552.1+2020	0.222	15.81	44.99	42.94	2.06	16.44	1	8.93
1555+111	PG 1553+11	0.360	15.42	46.38	44.10	5.07	>20.99	2	7.25
1602+308	RXS J1602.2+3050	0.302	15.34	44.64	43.64	1.85	...	...	...
1626+352	RXS J1626.4+3513	0.497	15.24	45.08	43.67	2.53	>17.89	1	9.22
1644+457	RXS J1644.2+4546	0.225	15.44	44.63	43.52	1.95	16.74	1	8.79
1652+403	RGB J1652+403	0.240	14.05	44.88	42.89	1.85	...	...	...
1653+397	MRK 501	0.034	15.96	44.63	41.68	4.79	12.51	1	8.72
1704+716	RXS J1704.8+7138	0.350	14.76	45.04	42.84	2.45	18.52	1	8.45
1719+177	PKS 1717+177	0.137	12.22	44.22	43.05	5.03	...	...	...
1724+400	B2 1722+40	1.049	14.44	46.38	45.66	4.72	...	...	...
1725+118	H 1722+119	0.170	15.86	45.46	43.38	2.57	>20.75	2	6.45
1728+502	IZw187	0.055	16.05	44.02	42.03	1.91	15.36	2	7.84
1739+476	OT 465	0.473	12.02	45.03	44.93	5.42	>19.75	2	8.22
1742+597	RGBJ 1742+597	0.400	13.85	45.24	43.51	3.73	18.67	1	8.55
1743+195	NPM1G +19.0510	0.084	15.46	44.20	42.26	3.19	14.14	1	8.93
1745+398	B3 1743+398B	0.267	16.01	45.11	44.40	1.69	16.22	1	9.26
1747+469	B3 1746+470	1.484	12.50	46.15	45.10	11.33	...	...	...
1748+700	S4 1749+70	0.770	13.42	46.26	44.49	9.94	>17.68	2	9.90
1749+433	B3 1747+433	0.473	13.61	45.26	44.48	4.46	...	...	...
1750+470	RXS J1750.0+4700	0.160	17.05	44.12	43.14	0.72	16.33	1	8.58
1751+096	PKS 1749+096	0.322	11.81	45.83	42.78	37.09	17.93	2	8.64
1756+553	RXS J1756.2+5522	0.271	16.47	44.97	42.50	1.84	...	...	...
1757+705	MS 1757.7+7034	0.407	13.17	45.20	42.51	3.02	18.93	2	8.44
1800+784	S5 1803+784	0.680	13.41	46.72	45.35	8.51	>19.51	2	8.82
1806+698	3C 371	0.051	14.18	44.28	43.75	1.79	14.07	1	8.39
1808+468	RGB J1808+468	0.450	14.29	45.14	43.63	2.80	19.22	1	8.42
1811+442	RGB J1811+442	0.350	15.99	44.70	43.70	0.79	17.58	1	8.92
1813+317	B2 1811+31	0.117	14.85	44.09	42.81	1.73	17.66	1	7.55
1824+568	4C 56.27	0.664	12.40	46.14	45.88	4.07	18.88	2	9.10
1829+540	RXS J1829.4+5402	0.302	14.61	44.81	43.51	1.34	...	...	...
1838+480	RXS J1838.7+4802	0.300	13.65	45.09	43.33	2.45	18.61	1	8.22
1841+591	RGB J1841+591	0.530	14.34	44.93	43.46	1.44	18.08	1	9.21
1853+672	1ES 1853+671	0.212	13.07	44.19	41.67	3.00	17.83	2	8.18
1927+612	S4 1926+61	0.473	12.70	45.67	44.43	7.66	...	...	...
1959+651	1ES 1959+650	0.047	15.87	44.54	40.89	5.20	14.40	2	8.14
2005+778	S5 2007+77	0.342	12.80	45.46	44.00	7.70	18.16	2	8.60
2009+724	S5 2010+72	0.473	12.79	45.23	44.80	7.45	...	...	...
2022+761	S5 2023+76	0.473	14.49	45.77	44.43	5.39	...	...	...
2039+523	1ES 2037+521	0.053	14.78	44.31	40.15	3.55	13.65	2	8.65
2134−018	PKS 2131−021	1.285	12.10	46.66	45.78	11.93	>18.94	2	9.96
2145+073	MS 2143.4+0704	0.237	13.56	44.67	42.99	2.53	17.42	2	8.52
2152+175	PKS 2149+17	0.473	12.57	45.35	43.88	10.39	>20.63	2	7.78
2202+422	BL LAC	0.070	13.58	45.05	42.08	14.47	14.42	2	8.58
2250+384	B3 2247+381	0.119	15.05	44.64	42.51	2.03	15.51	1	8.64
2257+077	PKS 2254+074	0.190	13.03	45.07	42.63	8.85	16.22	2	8.85
2319+161	Q J2319+161	0.302	15.34	44.90	43.41	2.00	...	...	...
2322+346	TEX 2320+343	0.098	15.18	44.30	42.41	1.23	14.88	1	8.73
2323+421	1ES 2321+419	0.059	14.21	43.76	41.39	1.70	...	...	...
2329+177	1ES 2326+174	0.213	16.57	44.89	42.92	2.04	17.17	2	8.51
2339+055	MS 2336.5+0517	0.740	14.78	46.57	44.01	1.82	...	...	...
2347+517	1ES 2344+514	0.044	15.50	44.23	41.18	3.63	13.39	2	8.57
2350+196	MS 2347.4+1924	0.515	15.88	45.15	43.07	1.81	...	...	...

Notes: Col. 1: the source IAU name (J2000). Col. 2: the source alias name. Col. 3: the redshift. Col. 4: the intrinsic synchrotron peak frequency. Col. 5: the observed peak luminosity in units of $\rm erg\ s^{-1}$. Col. 6: the jet power in units of $\rm erg\ s^{-1}$. Col. 7: the Doppler factor. Col. 8: the R magitude of host galaxies. '>' indicates the lower limit. Col. 9: the references of $m_{\rm h}$: 1, Nilsson et al. (2003); 2, Urry et al. (2000); 3, Nilsson et al. (2007); 4, O'Dowd & Urry (2005). Col. 10: the black hole mass in units of solar mass.

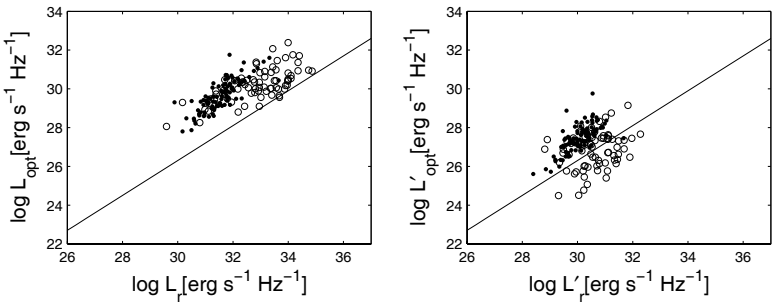

Fig. 1 The optical vs. radio core luminosity. The solid line is the best fit of the correlation found by Chiaberge et al. (1999) for FR I nuclei. The open circles represent LBLs, while the filled circles are for IBLs and HBLs. In the left panel, the observed luminosities are shown, while the debeamed luminosities with $\Gamma = 5$ for a mean viewing angle of 60° are used in the right panel (see text for details).

3.1 Radio and Optical Core Luminosity

We plot the observed radio and optical core luminosities in the left panel of Figure 1, together with the best fit (the solid line) of the correlation found by Chiaberge et al. (1999) for FR I nuclei. The objects in the present sample span about five orders of magnitude in the radio core luminosity, and the optical core luminosity increases linearly with it over this range. There is a significant correlation between the radio and optical core luminosities at $\gg$99.99% level, which is confirmed by the partial correlation analysis that excludes the common dependence on the luminosity distance. This correlation suggests that the emission at two wavebands is ascribed to the same non-thermal process, just as in FR I radio galaxies. However, we find that the points are all above the fitted line of Chiaberge et al. (1999), and the optical core luminosities are brighter by about two orders of magnitude than those of FR I nuclei, at the same radio core luminosities.

We correct the beaming effect for the radio and optical core luminosity with the estimated Doppler factor. The intrinsic optical core luminosities are estimated assuming $\alpha_{\rm o} = 1$ (Falomo et al. 1994), while we use $\alpha_{\rm r} = 0.0$ in the radio band. We also recalculated the luminosities in the hypothesis of a bulk Lorentz factor of $\Gamma = 5$ and a viewing angle of 60°, which is the average angle expected for the population of FR I radio galaxies used by Chiaberge et al. (1999) to derive the correlation. The recalculated luminosities are presented in the right panel of Figure 1. It is apparent that the data points move toward the lower radio and optical luminosities due to the debeaming. Although with some scatter, the debeamed radio and optical luminosities follow the correlation of Chiaberge et al. (1999) for FR I nuclei. This supports a common nature of BL Lac objects and FR I radio galaxy nuclei, which is consistent with the results of Giroletti et al. (2006) from the study of 29 nearby BL Lac objects.

3.2 Synchrotron Peak Frequency and Luminosity

In the left panel of Figure 2, we present the relationship between the observed peak luminosity $\nu L_{\nu_{\rm peak}}$ and synchrotron peak frequency $\nu_{\rm peak}$, while the relationship of the intrinsic parameters $\nu L_{\nu'_{\rm peak}}$ and $\nu'_{\rm peak}$ is shown in the right panel. We find a weak negative correlation between $\nu L_{\nu_{\rm peak}}$ and $\nu_{\rm peak}$. In contrast, after correcting the beaming effect both in the peak luminosity and synchrotron peak frequency, we find a significant positive correlation between $\nu L_{\nu'_{\rm peak}}$ and $\nu'_{\rm peak}$ with a Spearman correlation coefficient of $r = 0.59$ at $\gg$ 99.99% confidence level. It should be noted that this correlation may be caused by the common dependence of both parameters on the Doppler factor, as $L_{\rm int} = L_{\rm obs}/\delta^{2+\alpha}$ ($\alpha = 1$ in this case) and $\nu'_{\rm peak} = \nu_{\rm peak}/\delta$. We therefore use the partial Spearman correlation method (Macklin 1982) to check this correlation. Still, a significant correlation with a correlation coefficient of 0.33 is present at 99.99% significance level between $\nu L_{\nu'_{\rm peak}}$ and $\nu'_{\rm peak}$, independent of the Doppler factor. To further check this correlation, we also perform a statistical analysis of the sources in the re-

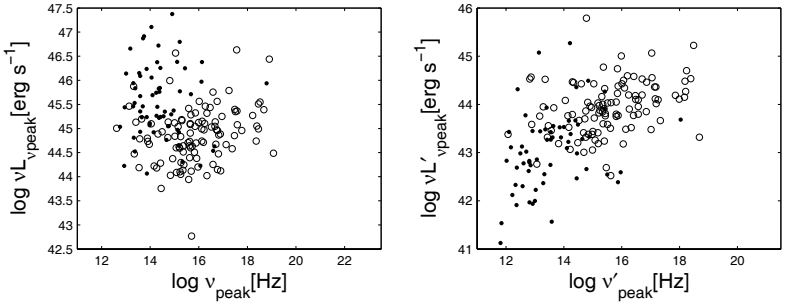

Fig. 2 The peak luminosity versus synchrotron peak frequency. The left panel is for observed values, while the intrinsic ones are shown in the right panel. The open circles represent the sources with Doppler factor $\delta < 3.5$ (see text for details).

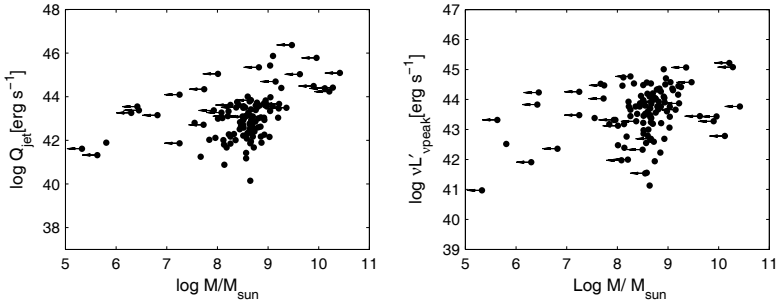

Fig. 3 Left: the black hole mass versus the jet power. Right: the black hole mass versus the intrinsic luminosity at synchrotron peak frequency. The arrows indicate the upper limit of black hole mass.

stricted Doppler factor range δ <3.5. In this subsample of sources, there is no correlation between the Doppler factor and $\nu'_{\rm peak}$, while a significant correlation is still present between $\nu L_{\nu'_{\rm peak}}$ and $\nu'_{\rm peak}$ with a Spearman correlation coefficient of r=0.37, at over 99% significance level (see Fig. 2). Therefore, we conclude that the positive correlation between the intrinsic peak luminosity and intrinsic peak frequency might be intrinsic, at least for our present sample.

The intrinsic luminosity at the synchrotron peak frequency can be a good indicator of the jet emissions due to the fact that the majority of jet synchrotron emissions are radiated at the synchrotron peak frequency. Therefore, the significant positive correlation between $\nu L_{\nu'_{\rm peak}}$ and $\nu'_{\rm peak}$ implies that the jet emissions are closely related to the synchrotron peak frequency, which is only dependent on B and $\gamma_{\rm peak}$.

3.3 The Black Hole Mass and Luminosity

We estimated the black hole mass using the relationship between the R-band absolute magnitude of host galaxy $M_{\rm R}$ and the black hole mass $M_{\rm bh}$ proposed by McLure & Dunlop (2002):

$$\log\ M_{\rm bh} = -0.50\ M_{\rm R} - 2.96 \tag{4}$$

for 121 sources with available $M_{\rm R}$ from the literature. There are four sources without measured redshifts, which are excluded from the correlation analysis.

Figure 3 shows the correlation between the black hole mass and jet power (left), and intrinsic peak luminosity (right). The black hole mass of 34 sources is only given as an upper limit due to the faintness and the upper limit of the R-band magnitude of host galaxies. We used the astronomy Survival Analysis (ASURV) package (Isobe & Feigelson 1990; Lavalley et al. 1992) when we investigate the correlation

involving these upper limits. We find a strong correlation between the intrinsic peak luminosity $\nu L_{\nu'_{\rm peak}}$ and the black hole mass $M_{\rm bh}$ with a correlation coefficient of $r = 0.27$ at 99.7% confidence level, while there is originally no correlation between the observed peak luminosity and the black hole mass. The partial correlation analysis, which excludes the common dependence on redshift, still shows a significant correlation at 99.9% significance level. Moreover, we find a mild correlation between the jet power and the black hole mass at about 95% confidence level, which is also confirmed by the partial correlation analysis. These results imply that the sources with larger jet power and/or jet emission systematically possess heavier black holes.

4 DISCUSSION

It can be seen from Figure 2 that very high synchrotron peak frequencies exist in several objects with $\log \nu_{\rm peak} > 17$. Ghisellini et al. (1999) have suggested the existence of ultra-high-energy synchrotron peak BL Lacs (UHBLs), whose synchrotron peak frequencies lie at even higher frequencies than those of conventional HBLs, $\log \nu_{\rm peak} > 19$. In our sample, we find eight objects with $\log \nu'_{\rm peak} > 18$ (see Table 1), which thus can be potential UHBLs. However, as Nieppola et al. (2006) pointed out, using a simple parabolic function in the fitting may produce some errors, especially among HBLs, and the peak frequencies of the extreme objects can be exaggerated and cannot be considered as definite. Although there are no sources with extreme peak frequencies $\log \nu'_{\rm peak} > 19$ in our sample, we conservatively re-examine our results after excluding all eight sources with $\log \nu'_{\rm peak} > 18$. We find that it does not alter our results.

We note that Equation (1) used to estimate the Doppler factor is based on the assumption of a Lorentz factor of five (Giovannini et al. 2001). As Giovannini et al. (2001) claimed, a similar correlation can be obtained for Γ in the range 3–10, so generally Equation (1) can be extensively used in this range. However, the simplification of a similar Lorentz factor in a sample may produce errors in the estimated Doppler factor. As a matter of fact, the superluminal motion studies (Vermeulen & Cohen 1994; Jorstad et al. 2001, 2005) showed that some LBLs may have large apparent velocities, $> 10c$ in some cases, which implies that their Lorentz factors are larger than 10. We collected the available apparent velocity for 27 sources in our sample from literatures, and find that the median value is about $3c$, and only three sources have apparent velocities larger than $10c$. As BL Lac objects are normally viewed at small viewing angles, the Lorentz factor can be roughly constrained if we assume the viewing angle $\theta = 1/\Gamma$. We find that the median value of the constrained Lorentz factor is right in the range 3–10. Moreover, utilizing the variability in the Doppler factor and apparent velocity, Lähteenmäki & Valtaoja (1999) and Valtaoja et al. (1999) showed that the averaged lorentz factors of radio selected BL Lac objects are around 5. In addition, Gabuzda et al. (2000) found no evidence that the typical jet Lorentz factor exceeds $\Gamma \sim 5-6$ from the apparent superluminal speed distribution of 16 northern BL Lac objects. We thus conclude that the assumption of a Lorentz factor of 5, or a range of 3–10 is a good approximation although some exceptions do exist. We find that the sources with large apparent velocities are mainly LBLs. If these sources do have Lorentz factors larger than ten, our method may likely underestimate the Doppler factor. Adopting a real Doppler factor may produce a smaller intrinsic synchrotron luminosity than ours, which, however, may strengthen our results since these sources will be vertically lower in the LBL region in Figure 2.

The 'blazar sequence,' power - $\nu_{\rm peak}$ anti-correlation, was originally presented by Fossati et al. (1998) based on one radio- and one X-ray-selected sample of BL Lacs, and one FSRQ sample. These samples have been assembled in an independent and somewhat different way, especially regarding the selection band, and indeed none of the individual samples in figure 7 of Fossati et al. (1998) showed the claimed anti-correlation between power and $\nu_{\rm peak}$, which was only apparent by combining the three samples (Padovani 2007). The blazar sequence was recently tested by Nieppola et al. (2008). After eliminating the beaming effect of peak frequencies and luminosities, Nieppola et al. (2008) found that the blazar sequence disappears. Instead, for BL Lac objects separately, they found a positive correlation between the synchrotron peak frequencies and luminosities. Intriguingly, this is consistent with our results. The blazar sequence thus can be an observational phenomenon created by variable Doppler

boosting across the synchrotron peak frequency range (Nieppola et al. 2008). By now, what really determines the shifting of the synchrotron peak frequency still seems unclear. Wang et al. (2002) claimed that the shape of SEDs is related to the accretion rate in BL Lac objects. They found that HBLs and LBLs follow the different anti-correlation between the peak frequency and accretion rate, which may indicate differences in the physical processes associated with the jets. We re-studied their results by collecting the emission line flux and using the intrinsic peak frequency for our samples. We found that the overall relation between the peak frequency and accretion rate is similar to their results. However, the separate correlations in HBLs and LBLs are not evident. The difference may be partly because we are using the intrinsic peak frequency. On the other hand, the number of BL Lac objects with the detected emission lines is still limited.

For a BL Lac sample, the luminosity at any fixed waveband actually represents a different portion of source SED because of the changing $\nu_{\rm peak}$ in the sources. Therefore, the dependence between the source luminosity and synchrotron peak frequency might be necessarily checked at the synchrotron peak frequency, at which most of the jet radiation is emitted. Moreover, it is necessary to debeam the luminosity, which is Doppler boosted due to the relatively small viewing angles of the jets. The strong positive correlation between the intrinsic peak luminosity and the intrinsic synchrotron peak frequency implies that the intrinsic source luminosity does depend on the location of the synchrotron peak, although with a large scatter. It seems that the higher peaked BL Lac objects are intrinsically more powerful than the low frequency peaked BL Lac objects in the present sample. Since $\nu'_{\rm peak} \propto \gamma^2_{\rm peak} B$, our results show that the power of jet emission increases with the magnetic field and electron Lorentz factor. This, however, is hard to explain by the existing models which advocate that the SED of relativistic jets is strongly affected by the (external) radiation field (e.g. Ghisellini et al. 1998). It may be possible that the cooling process is not important in BL Lac objects. As a matter of fact, the cooling in BL Lac objects is expected to be smaller than that in Flat Spectrum Radio Quasars (FSRQs) which have strong broad emission lines. Alternatively, the efficient injection of the fresh high energy electrons can be maintained for a certain time, although the cooling process can not be ignored. In any case, theoretical models should be developed to explain our results. It may also be important if we could measure the magnetic field for individual sources.

We note that the strong-lined counterparts of HBLs, i.e. FSRQs with high $\nu_{\rm peak}$ have also been discovered in DXRBS by Padovani et al. (2003). Solely with DXRBS, they found no anti-correlation between synchrotron peak frequency and radio, BLR and jet power, contrary to the predictions of the blazar sequence scenario. Due to the great similarities between FSRQs and BL Lacs, it might be crucial to revisit our results with a large and complete sample including both BL Lacs and FSRQs, which will help us understand the physics of the dependence between the source luminosity and synchrotron peak frequency, jet formation.

5 CONCLUSIONS

By eliminating the beaming effect with the estimated Doppler factor from the radio data (Wu et al. 2007), we have calculated the intrinsic luminosity and the intrinsic synchrotron peak frequency for a sample of 170 BL Lac objects. Moreover, we estimated the black hole mass for our sample. The results can be summarized as follows:

1. After correcting the beaming effects, the radio and optical core luminosities follow with small scatter in the same correlation found for FR I radio galaxies by Chiaberge et al. (1999), which is in support of the unification of BL Lac objects and FR I galaxies based on orientation.
2. We find a significant positive correlation between the intrinsic luminosity at synchrotron peak frequency and the intrinsic synchrotron peak frequency. The result implies that the jet emission is closely related to the synchrotron peak frequency.
3. After correcting for the beaming effect, we find a strong correlation between the black hole mass and the peak luminosity, and a mild correlation in the case of jet power. The results indicate that the more powerful jets may have more massive black holes.

Acknowledgements We thank the anonymous referee for insightful comments and constructive suggestions. We thank Xinwu Cao for helpful discussions and suggestions. This work is supported by the NSFC under grants 10373019, 10633010 and 10703009. The National Radio Astronomical Observatory is operated by Associated Universities, Inc., under a cooperative agreement with the National Science Foundation. MERLIN is a National Facility operated by the University of Manchester at Jodrell Bank Observatory on behalf of PPARC. This research made use of the NASA/ IPAC Extragalactic Database (NED), which is operated by the Jet Propulsion Laboratory, California Institute of Technology, under contract with the National Aeronautics and Space Administration. This work also made use of Astrophysical Catalogs Support System (CATS) maintained by the Special Astrophysical Observatory, Russia.

References

Bauer, F. E., Condon, J. J., Thuan, T. X., & Broderick, J. J. 2000, ApJS, 129, 547
Capetti, A., Celotti, A., Chiaberge, M., et al. 2002, A&A, 383, 104
Chiaberge, M., Capetti, A., Celotti, A., et al. 1999, A&A, 349, 77
Donato, D., Ghisellini, G., Tagliaferri, G., & Fossati, G. 2001, A&A, 375, 739
Lähteenmäki, A., & Valtaoja, E. 1999, ApJ, 521, 493
Falomo, R., Scarpa, R., & Bersanelli, M. 1994, ApJS, 93, 125
Fossati, G., Maraschi, L., Celotti, A., Comastri, A., & Ghisellini, G. 1998, MNRAS, 299, 433
Gabuzda, D. C., Pushkarev, A. B., & Cawthorne, T. V. 2000, MNRAS, 319, 1109
Ghisellini, G. 1999, ApL&C, 39, 17
Giommi, P., Ansari, S. G., & Micol, A. 1995, A&AS, 109, 267
Giommi, P., Piranomonte, S., Perri, M., & Padovani, P. 2005, A&A, 434, 385
Giovannini, G., Cotton, W. D., Feretti, L., Lara, L., & Venturi, T. 2001, ApJ, 552, 508
Giroletti, M., Giovannini, G., Taylor, G. B., & Falomo, R. 2006, ApJ, 646, 801
Ghisellini, G., Celotti, A., Fossati, G., Maraschi, L., & Comastri, A. 1998, MNRAS, 301, 451
Jorstad, S. G., Marscher, A. P., Mattox, J. R., et al. 2001, ApJ, 556, 738
Jorstad, S. G., Marscher, A. P., Lister, M. L., Stirling, A. M., Cawthorne, T. V., et al. 2005, AJ, 130, 1418
Laurent-Muehleisen, S. A., Kollgaard, R. I., Feigelson, E. D., Brinkmann, W., & Siebert, J. 1999, ApJ, 525, 127
Nieppola, E., Tornikoski, M., & Valtaoja, E. 2006, A&A, 445, 441
Nieppola, E., Valtaoja, E., Tornikoski, M., Hovatta, T., & Kotiranta, M. 2008, A&A, 488, 867
Nilsson, K., Pursimo, T., Heidt, J., Takalo, L. O., Sillanpää, A., et al. 2003, A&A, 400, 95
Nilsson, K., Pasanen, M., Takalo, L. O., Lindfors, E., Berdyugin, A., et al. 2007, A&A, 475, 199N
O'Dowd, M., & Urry, C. M. 2005, ApJ, 627, 97
Padovani, P., & Giommi, P. 1995, ApJ, 444, 567
Padovani, P., Perlman, E. S., Landt, H., Giommi, P., & Perri, M. 2003, ApJ, 588, 128
Padovani, P. 2007, Ap&SS, 309, 63
Punsly, B. 2005, ApJ, 623, L9
Rector, T., & Stocke, J. T. 2003, AJ, 125, 2447
Reich, W., Fuerst, E., Reich, P., Kothes, R., & Brinkmann, W. 2000, A&A, 363, 141
Trussoni, E., Capetti, A., Celotti, A., Chiaberge, M., & Feretti, L. 2003, A&A, 403, 889
Turriziani, S., Cavazzuti, E., & Giommi, P. 2007, A&A, 472, 699
Urry, C. M., Scarpa, R., O'Dowd, M., Falomo, R., Pesce, J. E., & Treves, A. 2000, ApJ, 532, 816
Urry, C. M., & Padovani, P. 1995, PASP, 107 , 803
Valtaoja, E., Lähteenmäki, A., Teräsranta, H., & Lainela, M. 1999, IAU Circ., 159, 1999
Vermeulen, R. C., & Cohen, M. H. 1994, ApJ, 430, 467
Veron-Cetty, M. P., & Veron, P. 2000, ESOSR, 19, 1
Wang, J.-M., Staubert, R., & Ho, L. C. 2002, ApJ, 579, 554
Wu, Z. Z., Jiang, D. R., Gu, M. F., & Liu, Y. 2007, A&A. 466, 63